Biomaterials 49 (2015) 37–46

Contents lists available at ScienceDirect

Biomaterials

journal homepage: www.elsevier.com/locate/biomaterials

Novel human-derived extracellular matrix induces *in vitro* and *in vivo* vascularization and inhibits fibrosis

Marc C. Moore, Vittoria Pandolfi, Peter S. McFetridge*

J. Crayton Pruitt Family Department of Biomedical Engineering, University of Florida, JG-56 Biomedical Sciences Building, P.O. Box 116131, Gainesville, FL 32611-6131, USA

ARTICLE INFO

Article history:
Received 29 September 2014
Accepted 20 January 2015
Available online 11 February 2015

Keywords:
Angiogenesis
Arterial tissue engineering
Biomimetic material
Immunomodulation
Fibrosis

ABSTRACT

The inability to vascularize engineered organs and revascularize areas of infarction has been a major roadblock to delivering successful regenerative medicine therapies to the clinic. These investigations detail an isolated human extracellular matrix derived from the placenta (*h*PM) that induces vasculogenesis *in vitro* and angiogenesis *in vivo* within bioengineered tissues, with significant immune reductive properties. Compositional analysis showed ECM components (fibrinogen, laminin), angiogenic cytokines (angiogenin, FGF), and immune-related cytokines (annexins, DEFA1) in near physiological ratios. Gene expression profiles of endothelial cells seeded onto the matrix displayed upregulation of angiogenic genes (TGFB1, VEGFA), remodeling genes (MMP9, LAMA5) and vascular development genes (HAND2, LECT1). Angiogenic networks displayed a time dependent stability in comparison to current *in vitro* approaches that degrade rapidly. *In vivo*, matrix-dosed bioscaffolds showed enhanced angiogenesis and significantly reduced fibrosis in comparison to current angiogenic biomaterials. Implementation of this human placenta derived extracellular matrix provides an alternative to Matrigel and, due to its human derivation, its development may have significant clinical applications leading to advances in therapeutic angiogenesis techniques and tissue engineering.

Published by Elsevier Ltd.

1. Introduction

The ability to initiate and control angiogenesis in a determinant fashion would have a significant impact in a wide range of clinical applications including tissue engineering, regenerative medicine, *in situ* regeneration after myocardial infarction, and the inhibition of cancer. Most approaches to initiate angiogenesis innately and within biomaterials have either had limited success or are simply not transferable to the clinic due to their non-human or tumor-derivation, limited biomolecular composition in comparison to the native *in vivo* environment, or lack of genetic regulation as in the case of methods to control gene expression [1,2]. Further, once implanted these approaches often cause immunological reactions and fibrotic capsule formation that prevents coupling with the native vasculature. As such, a clinically applicable approach to induce and control angiogenesis remains an extremely high priority [3].

Angiogenesis is a complex process that is both location and stimuli dependent, and in each instance the capacity to modulate these processes may involve a unique combination of regulatory molecules [4,5]. Control of vessel formation is further complicated by different mechanisms of formation, with the two most understood being intussusception and sprouting [6,7]. Intussusception is characterized by the insertion of interstitial cellular columns into the lumen of preexisting vessels [8], and sprouting is characterized by endothelial cells sprouting toward an angiogenic stimulus in tissue previously devoid of microvessels [9]. The innate control of angiogenesis is complex with a significant number of regulatory molecules identified [10], with more likely to be discovered. This diversity has driven researchers to identify modulators that control vascular development for drug screening, regenerative medicine and direct clinical therapies [1].

Common models to study angiogenesis use non-human or human recombinant proteins, animal-derived stimulators, or are entirely dependent on the use of live animals for evaluation [11]. *In vivo* animal models are commonly used to study angiogenesis because they provide an accurate model that compares to the complexity of multiple biomolecular pathways that occur during vessel formation. Current *in vivo* angiogenesis models include the rabbit corneal neovascularization assay, the *in vivo/in vitro* chick chorioallantoic membrane assay, the zebrafish assay, and the rat

* Corresponding author. Tel.: +1 352 273 9325; fax: +1 352 273 9221.
E-mail address: pmcfetridge@bme.ufl.edu (P.S. McFetridge).

http://dx.doi.org/10.1016/j.biomaterials.2015.01.022
0142-9612/Published by Elsevier Ltd.

mesentery window assay. However, these models are primarily intended for molecular pathway studies and are not ideal for clinical translation due to interspecies differences [12,13].

When possible, *in vitro* angiogenesis models are chosen as they control complex biological phenomena by limiting the number of molecular species that are needed to represent the complexity that exists *in vivo*. For example, human-derived recombinant growth factors have been used *in vitro* to model angiogenesis, and are typically based on single modulators such as FGF, TGF-β, VEGF [14]. Further approaches have used drug delivery techniques to control the delivery of combinations of modulators [15,16]. These methods, while showing positive outcomes, lack the variety of cytokines and chemical gradients associated with the native *in vivo* environment [17]. As such, in order to replicate the complex molecular cascades that occur *in vivo*, it is hypothesized that a multifactorial approach is necessary in order to promote competent vascularization.

The murine derived basement membrane matrix (BMM) or 'Matrigel' assay has been the preferred *in vitro* angiogenesis model (although *in vitro* may more closely represent vasculogenesis mechanisms) as it brings a degree of *in vivo* complexity to an *in vitro* model and results appear to be more comparable to *in vivo* data. However, due to the derivation of Matrigel from Engelbreth-Holm-Swarm (EHS) mouse sarcoma cells the product is not clinically relevant and as such is limited to *in vitro* testing. Further limiting desirability is that production of Matrigel requires the sacrifice of large numbers of animals [18].

Given interspecies differences associated with animal-derived angiogenesis models [12,13], and the complexity of creating multi-protein formulations from human recombinant proteins, a robust human derived approach (consisting of multiple proteins at near physiological ratios) would be desirable. Such an approach would have a significant impact in mechanistic studies, drug screening, and most importantly numerous clinical applications. For example, organ and tissue regeneration is largely restricted due to the inability to vascularize developing constructs. The capacity to modulate angiogenic processes to represent the different mechanisms and stages of formation would provide an improved platform to characterize key molecules and molecular pathways during vascularization.

To date, the majority of successful attempts to induce angiogenesis innately and within bioengineered tissues have relied upon non-human animal compounds, such as Matrigel and other animal derived angiogenesis modulators [19]. Due to their human derivation and capacity to remodel and adapt to changing fetal demands, we hypothesized that full-term placentas would yield a material with a complex extracellular matrix component in addition to pro-angiogenic compounds at near physiological ratios [20]. Here, directed fractionation and separations techniques were used to isolate a matrix containing a complex of active angiogenic biomolecules. Then, using cell-seeded human placenta matrix (*h*PM) and *h*PM-dosed vascular graft bioscaffolds, the matrix was shown to induce *in vitro* vasculogenesis and *in vivo* angiogenesis, to significantly enhance capillary formation, and to inhibit implant fibrosis. In addition, by modulating cell densities within this matrix, specific control of the rate of microvessel maturation as well as selective modeling of microvessel network morphology was achieved.

2. Methods

2.1. Human placental matrix derivation

Full-term placental tissues were collected at the delivery suite at Shands Hospital at the University of Florida (Gainesville, FL) in accordance with UF IRB #642010 within 12 h of birth. The umbilical cords and fetal membranes were removed and the placenta was dissected into 2 cm cubes and frozen. 12 h after progressive freezing to −86 °C at a rate of −1 °C/min, the placental cubes were transported to a cold room maintained at 4 °C where the rest of the procedures were completed. In preparation of each *h*PM batch, placental tissue from 3 separate donors was pooled (100 g total) prior to sample homogenization. Once at 4 °C, 100 g of the tissue was mixed with 150 mL cold 3.4 M NaCl buffer (198.5 g NaCl, 12.5 ml 2 M tris, 1.5 g EDTA, and 0.25 g NEM in 1 L distilled water). The NaCl buffer/tissue mix was homogenized into a paste then centrifuged at 7000 RPM for 15 min and separated from the supernatant. This NaCl washing process was repeated two additional times, discarding the supernatant each time to remove blood.

Next, the pellet was homogenized in 100 mL of 4 M urea buffer (240 g urea, 6 g tris base, and 9 g NaCl in 1 L distilled water), stirred on a magnetic stirplate for 24 h, and then centrifuged at 14000 RPM for 20 min (Sorvall RC6+ Centrifuge, Thermo Scientific, NC, USA). The supernatant was removed and dialyzed using 8000 MW dialysis tubing (Spectrum Laboratories, Inc., CA, USA) placed in 1L of TBS (6 g tris base and 9 g NaCl in 1 L distilled water) and 2.5 ml of chloroform for sterilization. The buffer was replaced with fresh TBS 4 more times, each at 2 h intervals. Finally, contents of the dialysis tubes were centrifuged at 3000 RPM for 15 min (Allegra X-12R Centrifuge, Beckman Coulter, Inc., CA, USA) to remove polymerized proteins, and the supernatant (pink viscous matrix) was collected and stored at −86 °C until use.

2.2. Biomolecular composition analysis

Relative cytokine levels were determined using a sandwich immunoassay array from RayBiotech, Inc. (Human Cytokine Antibody Array C Series 1000, Inc, GA, USA). Chemiluminescence was detected using a Foto/Analyst Luminaryfx Workstation (Fotodyne Incorporated, WI, USA) and the signal intensities were measured using TotalLab 100 software (Nonlinear Dynamics, Ltd, UK). The relative abundance of basement membrane and immune related biomolecules was performed (with 4 pooled samples) by MSBioworks (Ann Arbor, MI) using nano LC/MS/MS with a Waters NanoAcquity HPLC (Waters, Milford, MA) system interfaced to a Orbitrap Velos Pro (ThermoFisher, Waltham, MA). Proteins were identified from primary sequence databases using Mascot database search engine (Boston, MA). Total protein content was determined using a micro BCA protein assay (Pierce, Rockford, IL), and measured at 562 nm using a Synergy II microplate reader (BioTek, Winooski, VT).

2.3. RT-PCR analysis of cells from hPM-induced vasculogenic networks

Relative angiogenic gene expression was determined using 384-well RT^2 Human Angiogenesis RT^2 Profiler PCR Arrays (PAHS-024A, Quiagen, CA, USA). ECs were detached from culture plates using Accutase (Innovative Cell Technologies, San Diego, CA) and immediately stored in 100 μl of RNA*later*. RNA was extracted using the RNeasy Mini Kit (Quiagen, CA, USA), and genomic DNA was digested using an RNase-Free DNase kit (Quiagen, CA, USA). Purified RNA was reverse transcribed to cDNA using the RT^{2}First Strand Kit (SA Biosciences, TX, USA) with incubation at 42 °C for 15 min followed by incubation at 95 °C for 5 min to stop the reaction. Next, cDNA was mixed with RT^2 SYBR Green Mastermix (SA Biosciences, TX, USA) and loaded into 384-well Human Angiogenesis PCR Arrays. Using the Bio Rad CFX384 Real-Time System (Bio-Rad, CA, USA) the loaded array plates went through a denaturation cycle for 10 min at 95 °C, 40 cycles of 30 s annealing/extension cycles at 60 °C, and finally melting curves were obtained by ramping from 60 °C to 95 °C at a rate of °C per second. Data was analyzed the -using $\Delta\Delta C_t$ method and the RT^2 Profiler PCR Array Data Analysis Template v4.0 software package (Quiagen, CA, USA).

2.4. Human umbilical vein endothelial cell isolation and smooth muscle cell culture

Endothelial cells were derived from human umbilical veins (collected from UF Health Shands Hospital, Gainesville, FL) by detachment from the vessels walls as previously described using a 1 mg/ml solution of bovine Type-I Collagenase (Gibco, Invitrogen, NY, USA) in phosphate buffered saline [21]. The primary derived human umbilical vein endothelial cells (HUVEC) were used between passages 1–3 for all experiments. For comparison between the control group and the hPM group, endothelial cells in both sample groups were cultured using complete EC media which was prepared by adding 25 ml of glutamine, 0.5 ml of hydrocortisone, 0.5 ml of ascorbic acid, 10 ml of FBS, and 1.25 μl of bFGF to 500 mL VascuLife Basal media (Lifeline, MD, USA). Human smooth muscle cells (ATCC PCS-100-012) were obtained from the ATCC and used between passages 5 and 10 (Manassas, VA), and cultured under standard conditions at 37 °C and 5% CO_2. SMC were cultured in standard culture media consisting of high-glucose Dulbecco's Modified Eagle Medium (DMEM) (HyClone, Rockford, IL) supplemented with 10% FBS (Gibco, Carlsbad, CA), and cells were detached from culture plates using Accutase (Innovative Cell Technologies, San Diego, CA). To compare the morphologies of SMC culture on Matrigel and hPM, cells were seeded at 40,000 cells/cm^2 and cultured with unsupplemented high-glucose Dulbecco's Modified Eagle Medium (DMEM) (HyClone, Rockford, IL).

2.5. Preparation of placenta matrix-derived angiogenesis assays

Unless otherwise stated, 32 μl of placental matrix was thawed and pipetted into each well of a 96 well plate. The matrix was evenly coated onto the bottom of each well using an orbital shaker at 30 RPM for 1 min. The coated plate was then incubated at 37 °C for 30 min. HUVEC were then plating by direct pipetting at 20000 cells/cm^2, 40000 cells/cm^2, or 80000 cells/cm^2. Multiple time points were investigated at each concentration including at days 1, 3, and 5. Thrombospondin-1 was tested as an angiogenesis inhibiting drug using final concentrations 0, 5, 10, 20, and 35 μg/μL diluted in endothelial cell media.

2.6. Morphological characterization of vasculogenic networks

Network formation was analyzed after staining at a concentration of 2 μg/mL Calcein AM (Invitrogen-Life Technologies, NY, USA) with Endothelial cell culture media. In a dark room, dyed cells were incubated at 37 °C, 5% CO_2 for 30 min, and then images were taken using a Zeiss Axiovert 200 inverted Fluorescence microscope (Zeiss, Thornwood, NY). Three independent experiments were performed for each sample group, 6 wells were run per experiment, and 3 fields per well (each 500 μm^2) were used for quantification. Images were analyzed to determine the tubule length, tubule width, branch points, and other meshwork characterizations using ImageJ 1.45s (NIH, Bethesda, MD). Branch points were assigned manually as the positions at every node where branches meet or tubules sprout, and tubule length was assessed by determining the curve length from branch point to connected branch point. Tubule width measurements were carried out in three different zones per tubule, with two zones each 10 μm from the start and end and one zone in the middle of the curve length. The percent area of coverage was determined by processing the images using the ImageJ function "binary >> convert to mask" followed by measurement of the "mean." In TSP-1 experiments, final values were normalized to no dose samples, calculated as the percentage of "1" values relative to the total count of pixel values, and given as "% area coverage".

For scanning electron microscopy analysis of morphology, microvessel networks grown on glass slides were fixed in 2.5% glutaraldehyde, washed in PBS, fixed in 1% osmium tetroxide solution, and progressively dehydrated in 25%, 50%, 75%, 85%, 95% and 3 × 100% ethanol solutions. Samples were then critical point dried, coated with gold/palladium, and imaged using a Hitachi S-4000 FE-SEM.

2.7. Human umbilical vein scaffold derivation and placental matrix incubation

Placentas were collected from UF Health Shands Hospital (Gainesville, FL) and HUVs were dissected using an automated method as previously described [22]. Dissected HUV samples were decellularized in a 1% SDS (Thermo Scientific, Rockford, IL) solution at a solvent/tissue mass of 20:1 (w:v). Samples were decellularized on an orbital shaker plate at 100 rpm for 24 h and then rinsed with PBS prior to incubation overnight at 37 °C in a 70 U/mL DNase I solution (Sigma–Aldrich, St. Louis, MO) in PBS. Sample were terminally sterilized using a 0.2% per acetic acid/4% ethanol (Sigma–Aldrich, St. Louis, MO) solution for 2 h and finally pH balanced (7.4) using PBS. Following decellularization, scaffolds were cut into 1.5 cm × 1.5 cm × 0.075 cm sheets, prefrozen to −85 °C, and then lyophilized using a Millrock bench top manifold freeze dryer (Kingston, NY) for 24 h at −85 °C under 10 mT vacuum. Immediately prior to cell seeding, scaffolds were incubated for 2 h in *h*PM, Matrigel, or PBS (control) and seeded.

2.8. Animal implant revascularization study

Male Sprague–Dawley rats (6 month old, 200 g) were purchased from Charles River Laboratories (Wilmington, MA, USA), and all procedures were approved by the University of Florida IACUC (UF#201207728). In a biological hood, terminally sterilized HUV scaffolds were incubated for 2 h in 5 mL of *h*PM, Matrigel, or PBS (control), respectively. Animals were anesthetized using isoflurane inhalation, and subcutaneous pockets were created on the left and right side of the back by blunt preparation with scissors. One scaffold was inserted into each subcutaneous pocket, and skin was sutured using 4-0 sutures (Coviden, Mansfield, MA). After 5 days implantation, animals were euthanized, and samples were removed for analysis.

To analyze capillary network formation, immediately after removal from the animal, fibrotic capsules were dissected with a scalpel and the HUV samples were placed onto glass slides. Top-down images of the semi-translucent scaffold sheets were taken using an Imager M2 light microscope (Zeiss, Oberkochen, Germany) with an Axiocam HRm digital camera (Zeiss, Oberkochen, Germany). To quantify cell migration and scaffold remodeling, tissue samples were embedded in Neg-50 frozen section medium, sectioned into 7 μm sections (Microm HM550 cryostat, Thermo Scientific, Waltham, MA), and stained using standard hematoxylin and eosin (H&E) staining (Richard-Alan Scientific, Kalamazoo, MI).

2.9. Statistics

Results are reported as mean ± standard deviation. Linear regression was performed using SPSS (IBM, Somers, NY). Rt-PCR data was analyzed using RT^2 Profiler PCR Array Data Analysis Software v3.2 (SABiosciences, Valencia, CA).

3. Results

3.1. Derivation and characterization of human placental matrix

After initial mechanical homogenization and centrifugation the *h*PM derivation technique utilized a urea step to linearize and solubilize molecules. This was followed by dialysis separations to remove urea and allow the biomolecules to refold into their original conformations (Fig. 1a). All steps of the derivation were performed in a cold room at 4 °C. The final solution was translucent, highly viscous, and consisted of proteins between 8 kD to 868 kD. *h*PM could be used to soak biomaterials or made into a thin-film for tissue culture assays (Fig. 1b, c). Reproducibility of *h*PM was assessed by analysis of standard deviation of the total protein content in n = 3 batches of *h*PM (with each batch created using equal masses of tissue from 3 separate donors) and shown to have a have a similar reproducibility and protein content to Matrigel (Fig. 1d). Scanning electron microscopy images show the surface

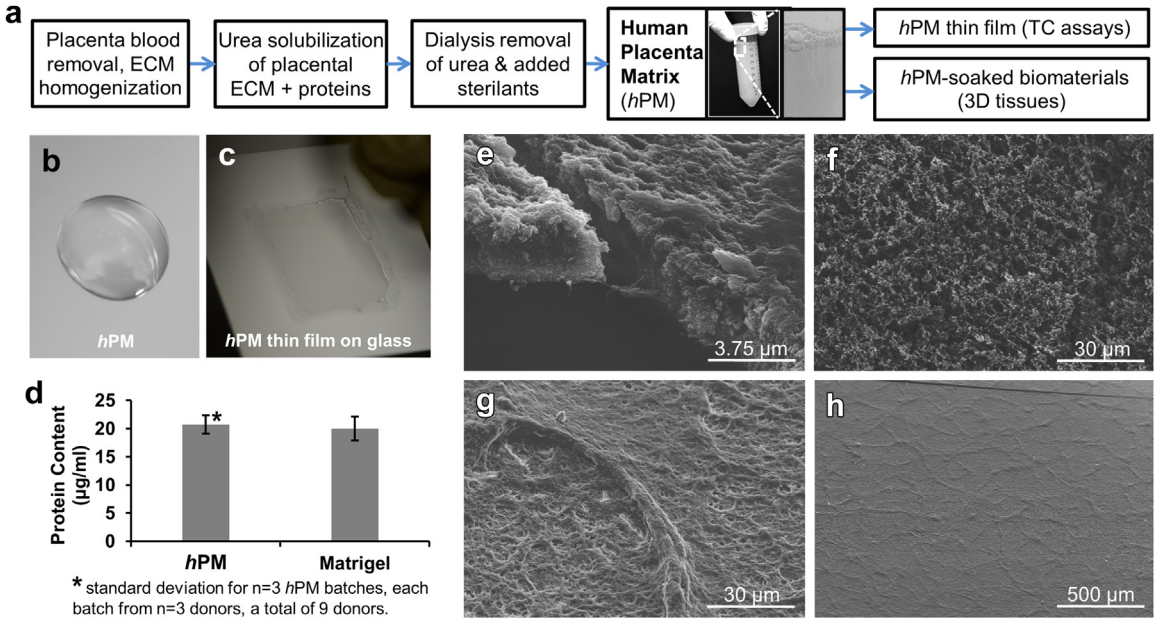

Fig. 1. *h*PM derivation and matrix morphology. (a) Human placenta matrix was obtained by homogenization of the placental ECM followed by urea solubilization and dialysis. (b) The final matrix was translucent and highly viscous allowing a variety of applications such as direct injection, coating porous/non-porous biomaterials or (c) made into thin films for tissue culture assays. (d) Reproducibility of *h*PM was assessed by analysis of standard deviation of the total protein content in n = 3 batches of *h*PM, with each batch created using equal masses of tissue from 3 separate donors (for a total of 9 donors). For comparison, protein content values of matrigel samples were also assessed. (e–f) SEM images show the surface morphology of *h*PM, and (g–h) vasculogenic network formation when HUVECS were seeded at 4 × 10^4 cells/cm^2 onto *h*PM thin films and cultured for 3 days.

morphology of *h*PM (Fig. 1e, f) and angiogenic network formation when HUVECS were seeded at 4 × 10^4 cells/cm^2 onto *h*PM thin films and cultured for 3 days (Fig. 1g, h).

Angiogenic potential of the matrix was initially characterized by seeding primary human umbilical vein endothelial cells (HUVEC) onto tissue culture plates (TCP) coated with the *h*PM. After 3 days of culture, cells had formed extensive angiogenic networks relative to control samples (Fig. 2a, b). Early stage cell and cording sprouting were visible within 1 h of cell seeding (data not shown), and angiogenic networks continued to mature until experimental termination at 3 d (Fig. 2c, d). The length of individual cell cords (multicellular) increased significantly from day 1 (Fig. 2e) to day 3 (Fig. 2f) of seeding.

Of 120 cytokines assessed, 54 angiogenesis related cytokines were detected in the placental matrix (Fig. 3a). The most prevalent angiogenesis related chemokine was angiogenin, which is a potent stimulator of new blood vessel formation [23]. Significant pro-angiogenic chemokines including hepatocyte growth factor (HGF), fibroblast growth factor-4 (FGF4), leptin (LEP), ICAM-1, ICAM-2 and TIMP-2 were also detected. LC-MS/MS showed the presence of immune related proteins including annexins (ANXA1, ANXA2, ANXA4, and ANXA5), neutrophil defensin (DEFA1), interleukin enhancer-binding factors (ILF2 and ILF3), IL27, ITBG1, and MRC1 (Fig. 3b). Basement membrane (BM) proteins associated with vessel formation were also detected using LC-MS/MS. These included, laminin (LAMA2, LAMA4, LAMA5, LAMB1, LAMB2, LAMB3, and LAMC1), fibronectin (FN1), heparin sulfate (HSPG2) and type-4 collagen (COL4A1, COL4A2, and COL4A3) (Fig. 3c), each of which has been shown to play key roles in angiogenesis [24–27].

3.2. Gene expression within hPM-induced angiogenic networks

In conjunction with chemokine analysis, HUVEC gene expression analysis further affirmed the angiogenic and vasculogenic nature of placenta matrix. RT-PCR analysis showed that endothelial cells seeded on *h*PM for 3 d expressed a wide range of essential pro-angiogenic genes including EGF, HGF, PGF, TGFB1 and VEGFA (Fig. 3d). The proteolytic enzymes MMP2 and MMP9, which play key roles in the degradation and remodeling of the surrounding extracellular matrix, as well as the facilitation of cell migration during angiogenesis were upregulated [28]. COLA4A, a key structural component of basement membranes during microvessel maturation, was also upregulated [29].

3.3. Capillary development and morphology in vitro

Historically, *in vitro* assays have little or no control over the rate and morphology of vasculogeneic network formations [11]. Data shows *in vitro* *h*PM-based vasculogenesis assays can be modulated to control the maturation and morphology of microvessel network formation by varying the initial cell seeding density. After 1 day, HUVEC seeded at density of 40,000 cells/cm^2 formed more defined tubules by comparison to seeding at a density of 80,000 cells/cm^2, but by day 5 cells at both seeding densities had formed well defined tubules (Fig. 4a). These results show the rate of network maturation is dependent on the initial seeding density.

Quantitative image analysis of the capillary networks (mean tubule length [mm], tubule density [#/mm^2], branch points [#/mm^2], meshes [#/mm^2], and mean tubule width [mm]) (Fig. 4b) showed that higher seeding densities resulted in a slower network

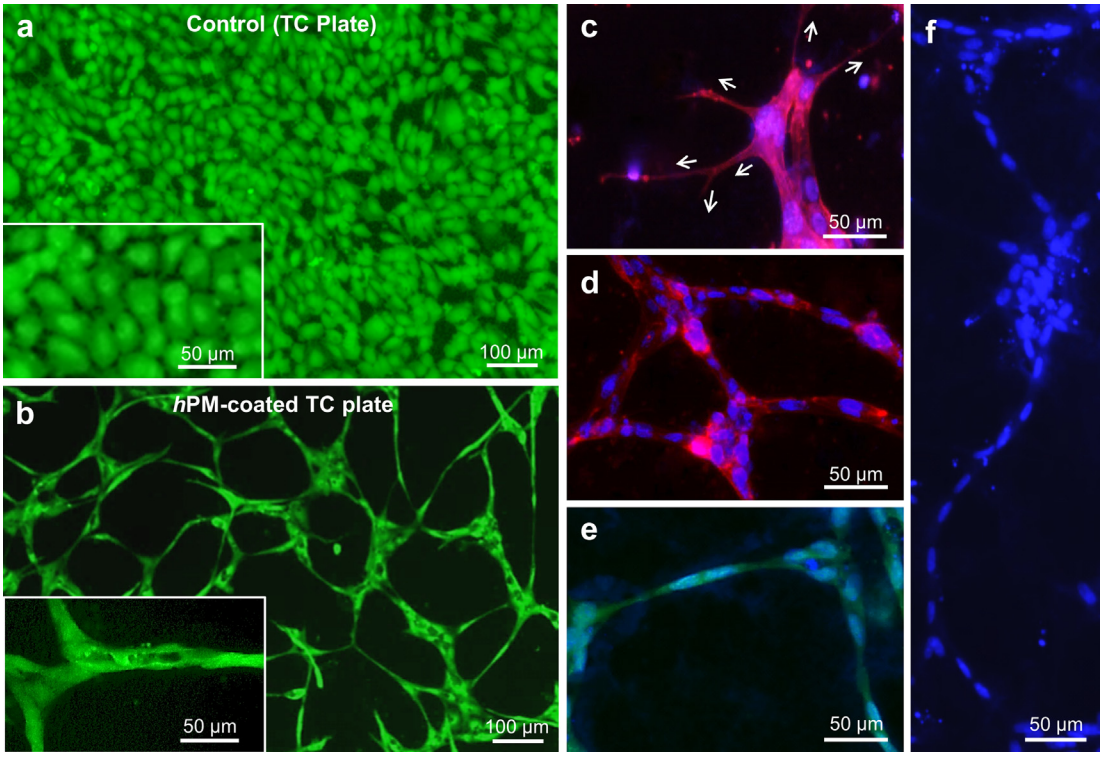

Fig. 2. Characterization of vasculogenic networks formed on *h*PM film. (a) HUVECs seeded onto a tissue culture plate at 4 × 10^4 cells/cm^2 and cultured in endothelial cell medium (control) for 3 d. (b) Formation of angiogenic networks by HUVECs seeded at 4 × 10^4 cells/cm^2 onto *h*PM-coated tissue culture plate (100 μL *h*PM/cm^2) and then cultured in endothelial cell medium for 3 d. (c) Rhodamine Phalloidin (red) and DAPI (blue) showing branched cell filopodia during angiogenic sprouting after 1 day on *h*PM. (d) Rhodamine Phalloidin (red) and DAPI (blue) showing a maturing angiogenic network with extensive cell cording after 3 days. (e) Calcein (green) and DAPI (blue) stained HUVEC during the initial stages of cell cording and vasculogenic network formation after 1 day on *h*PM. (f) DAPI (blue) staining showing cell cording of HUVEC after 3 d on *h*PM. (For interpretation of the references to color in this figure legend, the reader is referred to the web version of this article.)

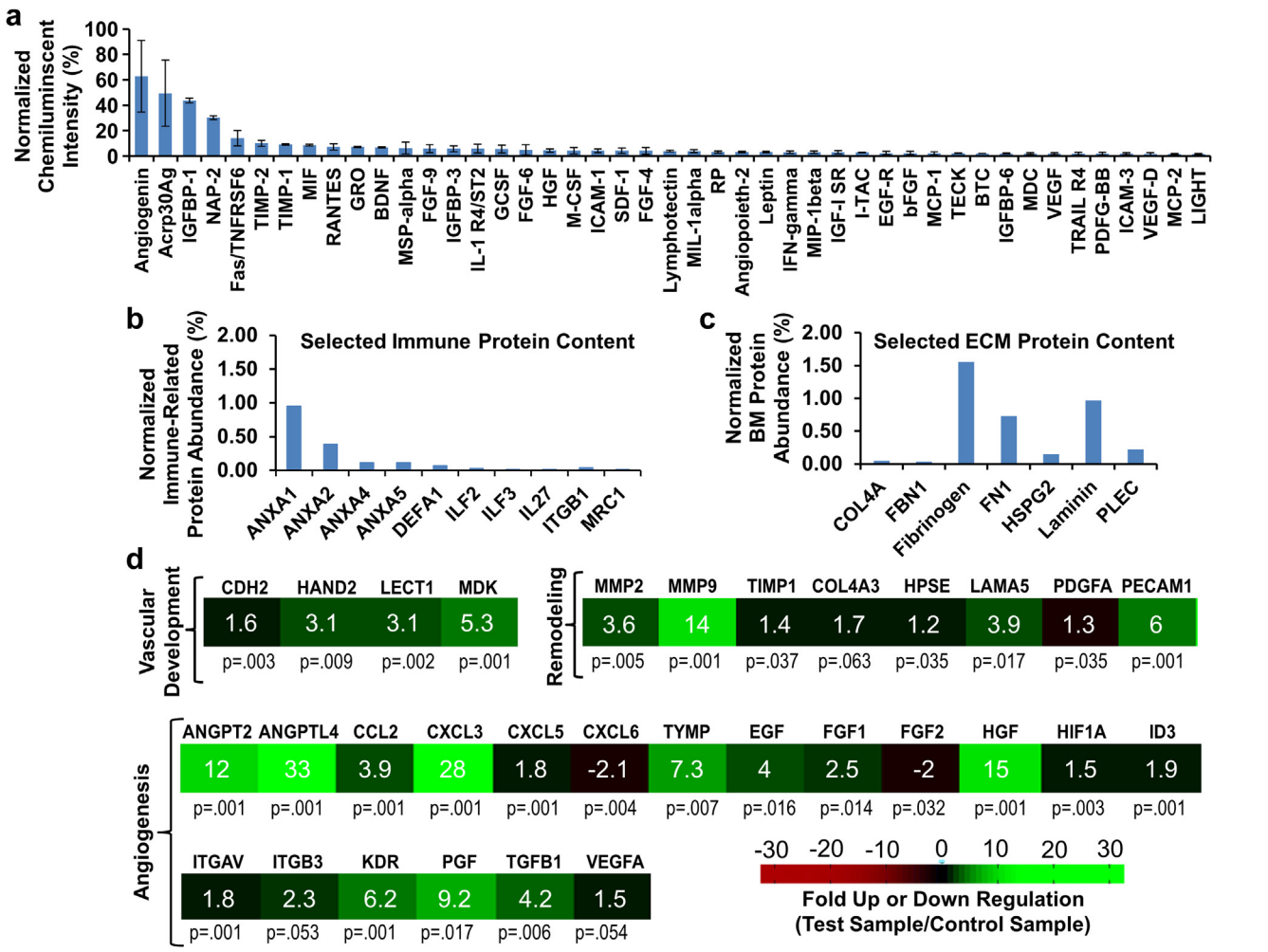

Fig. 3. Biochemical analysis of *h*PM and genetic analysis of HUVEC seeded on *h*PM. (a) Cytokines analysis was performed using a sandwich-based human angiogenesis antibody array, and data was normalized on a scale ranging from negative control values (0%) to positive control values (100%). Data are representative of 3 biological replicates. (b) Normalized spectral abundance factor (%) of immune-related and (c) angiogenesis-related BM related proteins was determined using 4 pooled samples analyzed using LC-MS/MS. Fibrinogen normalized spectral abundance factor is given as the sum of FGA and FGG values, and Laminin is given as the sum of LAMA2, LAMA4, LAMA5, LAMB1, LAMB2, LAMB3, and LAMC1 values. (d) Genetic analysis was performed on HUVECS seeded for 3 days onto 100 μL *h*PM/cm^2 at a density of 80,000 cells/cm^2. Some angiogenesis related proteins not present in the matrix, including placental growth factor (PGF), were upregulated by HUVECs when seeded onto *h*PM. Data are representative of four biological replicates. P-values are calculated using a Student's t-test of the replicate $2^{-\Delta Ct}$ values for each gene in the control group and treatment groups.

maturation (an extended time frame to reach the highest mean tubule length and number of meshes/mm^2), allowing a more detailed analysis as the time frame of network formation can be extended (data not shown). Comparatively, lower cell densities resulted in a faster maturation rate that would be more conducive to rapid screening approaches to (for example) test the effectiveness of angiogenesis blockers for cancer therapies.

As the historical gold standard for *in vitro* angiogenesis assays, microvessel networks induced by Matrigel were compared to *h*PM-induced networks (Fig. 4c). EC morphologies within capillary networks were first analyzed by exposing EC cultures to either Matrigel or *h*PM followed by assessment using Calcein AM to determine viability and network structure. Matrigel coated plates showed HUVEC to form defined vasculogenic tubule networks after 1 d, but after 3 d the same network structures collapsed into spherical balls of apoptotic cells (Fig. 4a, c). While some cell death was noted in *h*PM induced networks no apoptotic formations were observed after an extended 5 d period. During the late stages of angiogenesis EC recruit smooth muscle cells (SMC) to stabilize the growing micro-vessels. As such, the effect of *h*PM and Matrigel on smooth muscle cells morphology was assessed. Interestingly, in the absence of HUVEC, SMC seeded onto Matrigel formed tubules after 1 d, but on *h*PM coated plates SMC maintained typical 'hill and valley' formations (Fig. 4d), indicating significant differences in molecular signaling pathways between cell types.

3.4. Analysis of hPM induced vasculogenesis for drug screening applications

In addition to its role in regenerative medicine, vasculogenesis driven by *h*PM was tested for its ability to screen angiogenesis related drugs *in vitro*. Matrigel has been used extensively as a model for *in vitro* screening of anti-angiogenesis cancer drugs, and thus it was used as a control. The inhibition of vasculogenesis was assessed by comparison of EC cultured with Matrigel or *h*PM against TSP-1 (a glycoprotein with potent inhibition activity on angiogenesis and neovascularization) which represents a model drug for the anti-angiogenic treatment of solid tumors [30]. After 1 d of culture, control HUVEC were not affected by TSP-1, with cells forming typical cobblestone morphologies. By contrast vasculogenesis was significantly reduced when HUVEC dosed with TSP-1 were cultured on *h*PM treated culture plates (Fig. 5a). Results show the total

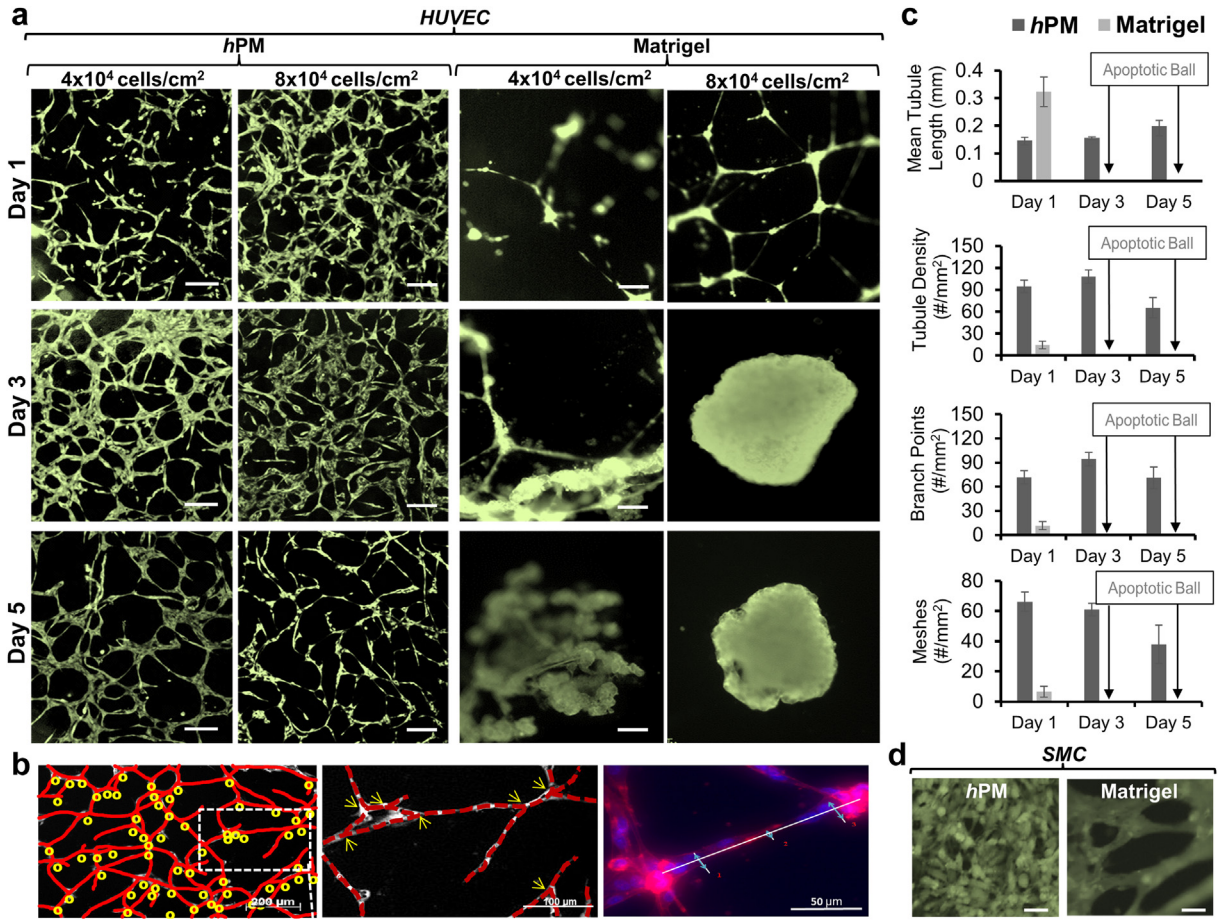

Fig. 4. *In vitro* vasculogenic networks formed on *h*PM and Matrigel coated tissue culture flasks. (a) Calcein stained HUVECS on *h*PM and Matrigel at variable cell seeding densities after 1 d, 3 d, and 5 d. The rate of vasculogenic network maturation, defined as the time until maximum number of tubules/mm^2, was modulated in *h*PM samples by varying cell seeding densities. In Matrigel samples, vasculogenic networks began to contract and form apoptotic balls after day 1. Scale bars, 200 μm. (b) Quantitative image analysis (masking) was used to determine angiogenic network parameters including mean tubule length (mm), tubule density (#/mm^2), number of branch points (#/mm^2), number of meshes (#/mm^2), and tubule width (mm). Analysis revealed that at 40,000 cells/cm^2 angiogenic networks took until day 3 to reach their maximum tubule density (tubules/mm^2), but at 80,000 cells/cm^2 networks reached their maximum tubule density in 1 day (data not shown). (c) Comparison of *h*PM and Matrigel induced vasculogenic network parameters showed that by day 1, in samples seeded at a density of 80,000 cells/cm^2, Matrigel samples had reach their maximum mean tubule length, tubule density, number of branch points, and number of meshes (with apoptotic ball formation by day 3), while *h*PM network parameters were more stable over 5 days of culture. (d) Primary human aortic smooth muscle cells (ATCC PCS-100-012) did not have vasculogenic formations when seeded for 3 days on *h*PM but did when seeded on Matrigel. Scale bars, 50 μm.

tubule-length and branch points to decrease linearly as a function of TSP-1 concentration in hPM samples, whereas Matrigel samples only show a low correlation over the assayed range of 0–35 μg TSP-1 per μL (Fig. 5b, c). These studies indicate *h*PM-based assays to be more sensitive to drug concentration compared to Matrigel-based assays. This is shown by the higher correlation between TSP-1 concentration and the reduction in coverage of the networks, with hPM and Matrigel assay R^2 values of 0.97 and 0.36, respectively (Fig. 5d). Importantly, the inhibition of network formation is further validation of actual vessel formation rather than an unknown stress response.

3.5. *In vitro* vasculogenesis within 3D bioscaffolds

Successful vascularization of engineered organs has been a major roadblock to developing successful regenerative medicine therapies [31,32], as such we analyzed the potential of *h*PM to induce vasculogenesis in an *ex vivo* derived bioscaffold. These studies show that scaffolds with adsorbed *h*PM induced the formation of vasculogenic networks within decellularized human umbilical vein bioscaffolds (Fig. 6a). Consistent with assays in 2D culture plates, EC seeded onto the bioscaffolds developed elongated morphologies that were connected into multi-cellular cords and formed complex interconnected networks. *In vivo* angiogenesis occurs predominantly by sprouting or intussusception mechanisms. Although angiogenesis and vasculogenesis are inherently different, EC seeded and cultured on *h*PM dosed 3D scaffolds displayed sprouting-like and intussusceptive-like mechanisms more commonly associated with angiogenesis. Initial tube formations were shown to be modulated by varying cell density where lower cell densities (2×10^4 cells/cm^2) network morphologies exhibited a mechanism of formation similar to sprouting angiogenesis (Fig. 6ci, cii), at intermediate densities (4×10^4 cells/cm^2) displayed formations similar to both sprouting-like and intussusceptive-like angiogenesis (Fig. 6ciii–cv) and at higher densities (6×10^4 cells/cm^2) formations similar to the intussusceptive mechanism of angiogenesis (Fig. 6cvi, cvii).

3.6. *Induction of angiogenesis in vivo*

Using a subcutaneous rat model (Fig. 7a) the angiogenic response to dosed scaffolds (Matrigel and *h*PM) was assessed after 5 days of implantation. Both control and Matrigel-dosed scaffolds displayed significant fibrosis surrounding the scaffold, whereas

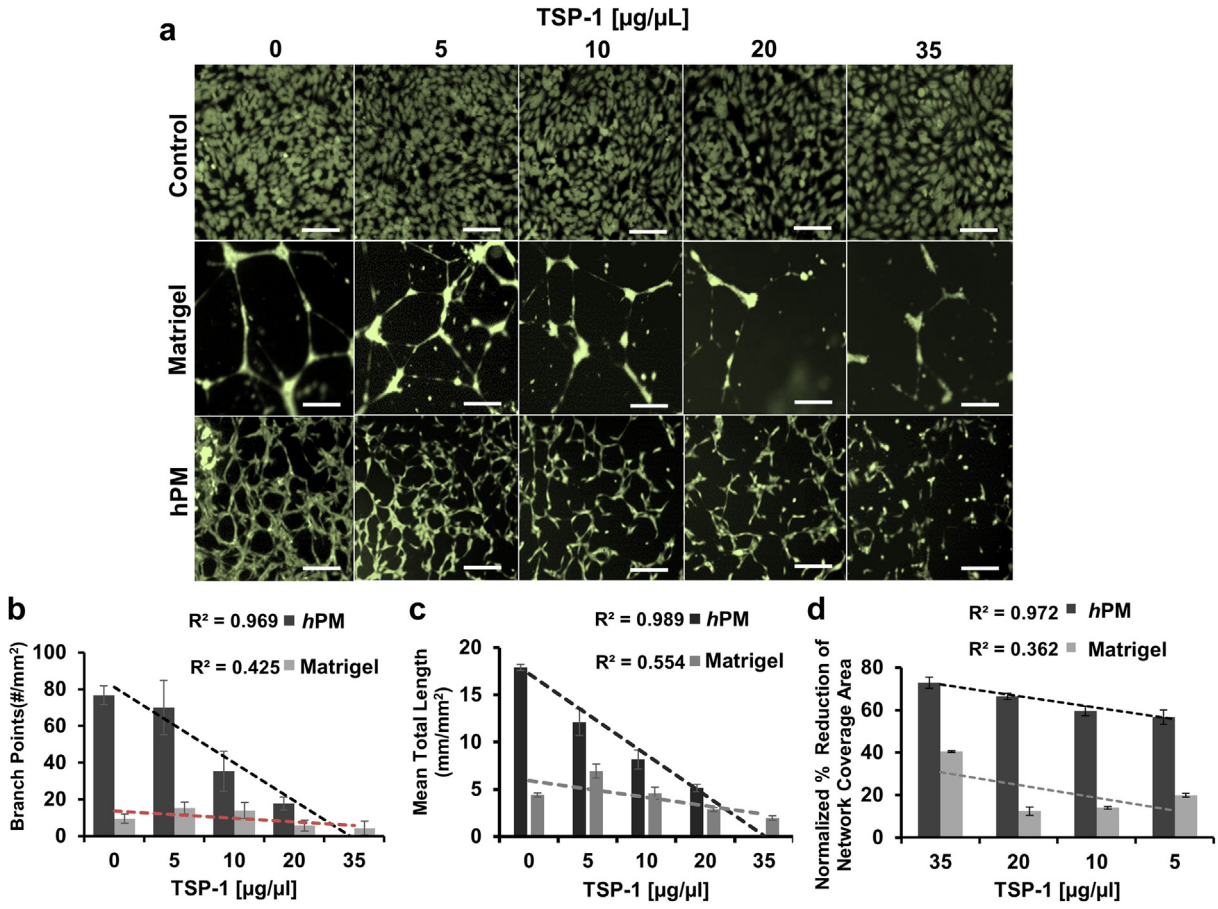

Fig. 5. Screening of anti-angiogenic tumor suppressive protein TSP-1 using an *h*PM-based angiogenesis assay. (a) HUVECS seeded onto *h*PM, Matrigel, and control culture flasks (not coated) for 1 day with TSP-1 (thrombospondin-1) added to the culture media were stained using Calcein AM. Scale bars, 200 µm. (b) In *h*PM-coated flasks, mean number of branch points (#/mm^2) and (c) total tubule length [mm/mm^2] both decreased linearly with increasing TSP-1 concentrations, whereas Matrigel samples only show a low correlation over the assayed range of 0–35 µg TSP-1 per µL. (d) Comparing normalized percent reduction of angiogenic network coverage area, *h*PM-coated culture plates had significantly higher sensitivity to TSP-1 concentration than Matrigel-coated culture plates, with R^2 values being 0.97 and 0.36, respectively.

*h*PM dosed scaffolds exhibited no discernable fibrosis (Fig. 7bi–biii). The inhibition of fibrosis in *h*PM samples was hypothesized to result from immune related molecules as detected with LC-MS/MS including anti-inflammatory Annexins (ANXA1, ANXA2, ANXA4, and ANXA5) [33], antimicrobial defensin peptides such as DEFA1 [34], and MRC1 which is known to bind to viral and bacterial pathogens [35].

As shown by brightfield microscopy, after 5 days implantation scaffolds dosed with Matrigel and *h*PM displayed a significant increase in neovascularization, with densities of 27.3 ± 2.7 tubules/mm^2 and 29.6 ± 4.1 tubules/mm^2, respectively compared to controls with densities of 2.4 ± 1.6 tubules/mm^2 (Fig. 7biv–bvi). While the total vascularization appeared similar between Matrigel and *h*PM treatments, the capillaries forming in Matrigel samples appeared less structured, without evidence of mature capillary bed formation. By comparison, *h*PM treated samples displayed capillaries beds with adjoining arterioles and venules (see inset Fig. 7bvi). H&E analysis of scaffold cross sections show cells migrated into and throughout scaffolds dosed with *h*PM, whereas Matrigel-dosed samples had comparatively reduced cellular infiltration, and cells within the control samples were limited to the scaffold periphery (Fig. 7bvii–bix). The more extensive cell migration in both Matrigel and *h*PM-dosed samples was attributed to chemotactic and growth factor signals adsorbed to the scaffold structure during incubation. Despite improved cell migration with both *h*PM and Matrigel dosed scaffolds over controls, cellular remodeling between the sample groups displayed significant variation. Cell dense regions in the Matrigel-dosed samples displayed remnants of the original HUV fibers (see inset Fig. 7bviii), with the general structure qualitatively more amorphous in comparison to *h*PM-dosed scaffolds that displayed more organized fiber and cellular structures (see inset Fig. 7bvix) as well as more extensive remodeling (Fig. 7bvii–bix).

4. Discussion

Tissue regeneration, infarct tissue and ischemic wound repair are three clinical areas where an improved strategy for wound recovery or organ replacement would have significant clinical impact [36]. The use of placental tissues in a variety of applications has grown significantly over the last 5 years, with an increasing body of evidence indicating they hold considerable clinical promise [22,37–39]. Results herein detail a novel human derived placental matrix (*h*PM) with naturally incorporated pro-angiogenic cytokines in near physiological ratios. These data show *h*PM to act as a potent human-derived stimulator of angiogenesis and tissue remodeling, with enhanced functional capillary formation (*in vitro* and *in vivo*) and a capacity to modulate vessel maturation. Additionally, *h*PM is shown to significantly reduce *in vivo* tissue fibrosis.

The capability of *h*PM to modulate the rate of capillary network formation and to control the morphology of angiogenic networks may provide a useful platform to further our understanding of

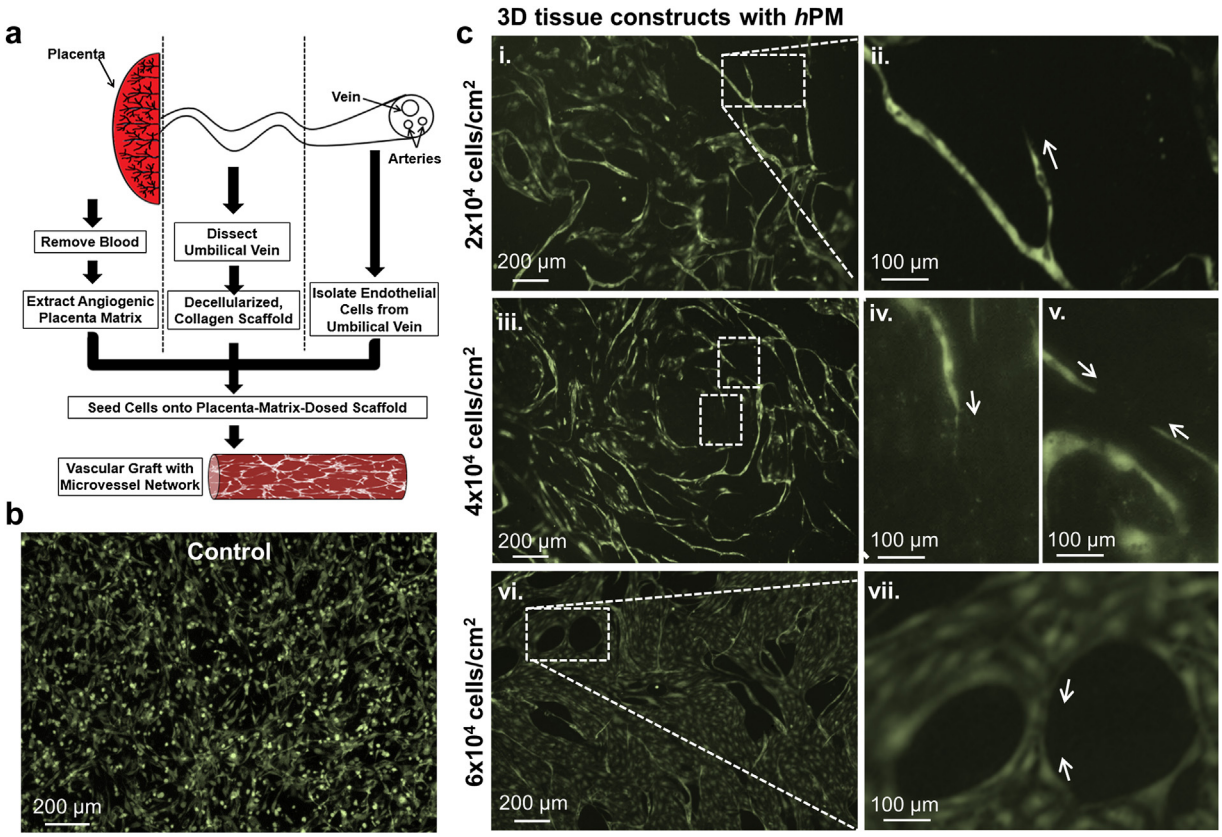

Fig. 6. *In vitro* vasculogenesis on 3D tissue constructs. (a) Using placental derived cells, scaffolds, and cytokines, vasculogenesis was induced *in vitro* in *h*PM-dosed (human umbilical vein) bioscaffolds after seeding and culturing for 3 days. (b) HUVEC seeded tissue scaffolds without *h*PM dosing did not form angiogenic networks. (c) Although vasculogenesis and angiogenesis are inherently different, representative images of *h*PM-dosed bioscaffolds show a mechanism of vasculogenesis after 3 days of culture that is similar to the sprouting and intussusceptive mechanisms of angiogenesis. (Ci–Cii) At a HUVEC cell seeding density of 20,000 cells/cm^2 a sprouting-like mechanism of network formation was most prevalent. (Ciii–Cv) At a seeding density of 40,000 cells/cm^2 occurrences of both sprouting-like and intussusceptive-like mechanisms of network formations were observed, whereas at (Cvi–Cvii) a density of 60,000 cells/cm^2 tubules formed via a mechanism that is similar to the intussusceptive mechanism of angiogenesis.

wound healing and organ regeneration. Similar to sprouting and intussusception mechanisms of angiogenesis, mechanisms associated with vasculogenesis were also observed, and shown to be dependent on initial cell density. Despite the inherent differences between angiogenesis and vasculogenesis, the correlation between cell density and the occurrence of sprouting-like and intussusceptive like mechanisms of vasculogenesis (in *h*PM assays) is similar to the current understanding of angiogenesis (*in vivo*). For example, sprouting is known to occur during early phases of angiogenesis in low cell density regions devoid of capillaries whereas intussusception occurs in higher cell density regions where capillaries preexist [40,41].

Matrigel has been used extensively to study angiogenesis and as a model for *in vitro* screening of anti-angiogenesis cancer drugs. The inhibition of angiogenesis was assessed by comparison of EC cultured with Matrigel or *h*PM against TSP-1, a potent inhibitor of angiogenesis [30]. Human EC exposed to *h*PM and TSP-1 elicited increased sensitivity with lower detection limits in comparison to Matrigel treated samples. Similarly, human SMC responded differently to Matrigel and *h*PM. Matrigel dosed SMC initiated capillary-like formations whereas SMC exposed to the *h*PM retained their typical hill and valley morphologies. SMC are not known to form tubules in the initial stages of microvessel formation, thus these results may indicate *h*PM-based angiogenesis more accurately models normal physiology. While similarities were noted with Matrigel in terms of driving cellular function, the mechanisms with which *h*PM stimulates cell function is likely to have significant differences, and as such requires further exploration.

Human-derived (recombinant) proteins have also been used to induce and model angiogenesis. These models typically rely on single or discrete combinations of angiogenesis modulators [42]. While discrete combinations are useful to control variation and reduce the inherent complexity of multifarious approaches, they constrain the screening process and fail to represent the broad set of human *in vivo* molecular interactions. It is hypothesized that regulation of only selected molecular pathways will confine attempts to induce competent angiogenesis as vessel formation *in vivo* requires the induction of multiple metabolic pathways [43,44]. This diversity is likely to play a significant role in replicating *in vivo* responses particularly when testing potential anti-angiogenesis or screening tumor suppressive drugs within the pharmaceutical industry. In comparison, the induction of angiogenesis by *h*PM uses a broad set of human-derived molecules at near physiological ratios. As such, a drug may modulate angiogenesis via interaction with any of these numerous pathways but may have little effect inducing competent angiogenesis as the complexity and regulatory pathways of the local environment are lacking.

Results from the *in vivo* analysis provide further evidence that the *h*PM complex influences multiple biochemical pathways resulting in a broad range of effects. Data shows *h*PM not only enhances angiogenic properties, but also has immune reductive properties, as illustrated by a negligible fibrotic response to *h*PM dosed bioscaffolds. Given the complex interactions between angiogenesis and the immune system [45], *h*PM provides a platform for the development of clinically applicable techniques to

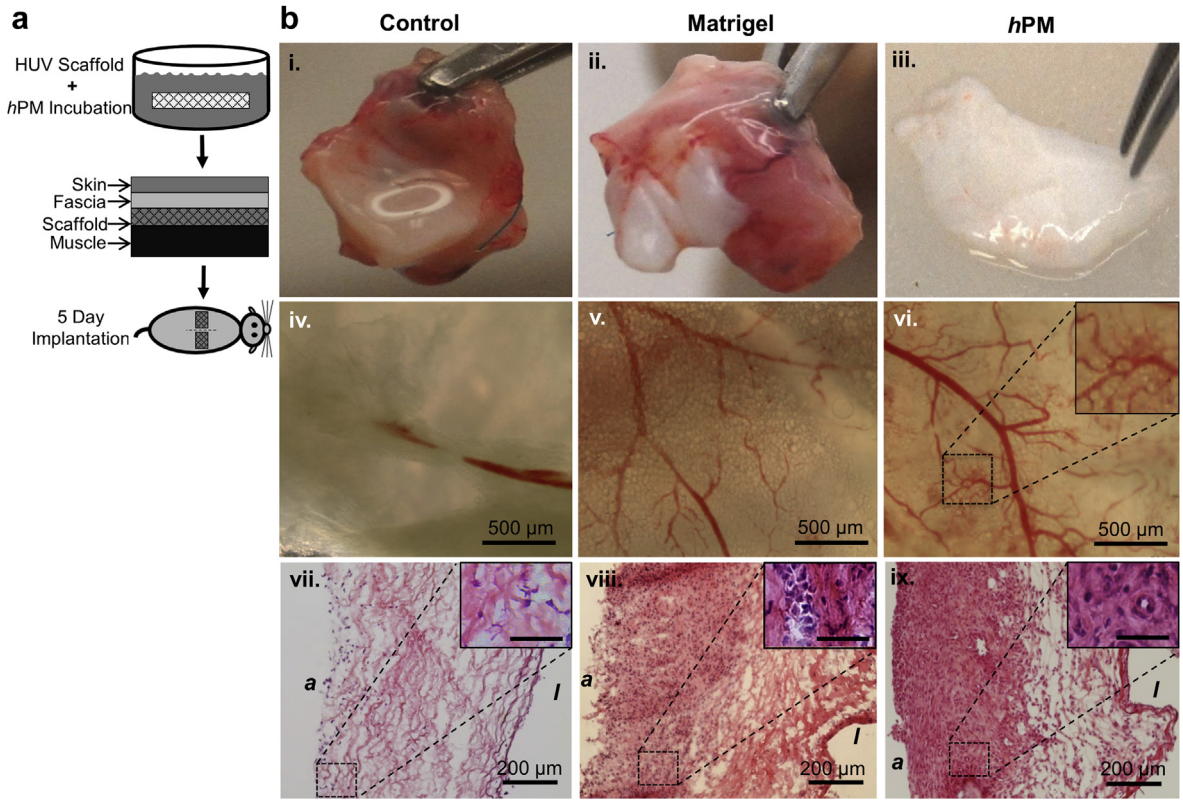

Fig. 7. *In vivo* angiogenesis in *h*PM dosed bioscaffolds. (a) Decellularized HUV scaffolds were incubated with *h*PM, Matrigel, or phosphate buffered saline (control) for 2 h prior to implantation into a rat model. Treated scaffolds were implanted between the fascia and muscle layers with the scaffold lumen adjacent to the fascia. (b) After 5 d implantation, scaffolds were removed for analysis. (bi–biii) Significantly more fibrotic capsule formation occurred in control and Matrigel-dosed bioscaffolds in comparison to *h*PM-dosed scaffolds. (biv–bvi) Brightfield images taken through the frontal plane of the semi-translucent bioscaffold sheets show that in comparison to controls, Matrigel-dosed and *h*PM-dosed scaffolds had significantly improved capillary network formation, with (bvi) the most mature capillary beds occurring in *h*PM-dosed scaffolds that formed vascular structures with connected arteriole to capillary to venule blood flow (indicated by dashed box). (bvii–bix) Hematoxylin and Eosin staining revealed that *h*PM-dosed scaffolds had the most scaffold remodeling in comparison to control and Matrigel-dosed scaffolds. (bvii) Control scaffolds had little remodeling of their original fiber orientation, and also the least cell migration into the scaffold from the abluminal surface of the HUV bioscaffold (indicated by italicized '*l*'). (bviii–bix) Matrigel-dosed scaffolds had reduced cell migration from the abluminal surface of the HUV in comparison to *h*PM dosed scaffolds. Cell distribution within Matrigel-dosed scaffolds was also less uniform with minimal structural remodeling in comparison to *h*PM-dosed scaffolds, which displayed modified collagen fiber orientation and a more uniform cell distribution.

induce capillary formation without significant immunological and inflammatory reactions. While considerable research is needed to further understand the complex mechanisms behind these results, our continuing hypotheses is that the positive outcomes are not only related to the presence of key growth factors (GF) and gene regulators but also their presence in physiological ratios obtained through the purification process. In comparison to models that rely on highly active and concentrated single GF, with many cases reporting undesirable results [46–48], these results show mature capillary bed formation with adjoining arterioles and venules [14,49,50]. Interestingly, while VEGF has been extensively studied as a key angiogenesis GF, and was upregulated in *h*PM induced EC, the original *h*PM composition of the solution contained no detectable levels indicating VEGF is only one of many contributing factors in vascular development. This contrasts Matrigel (BMM) that contains VEGF in both the standard and GFR (growth factor reduced) formulations.

Angiogenesis and vasculogenesis driven by *h*PM has been validated in 2D and 3D *in vitro* models, as well as within bioengineered tissue implants in a subcutaneous *in vivo* model. Its derivation from physiologically healthy, human neonatal vascular beds combined with its angiogenic and immune reductive properties make it unique among current angiogenesis models for both clinical and pharmaceutical applications. Further development in which discrete fractionations or compositions are optimized for specific mechanistic and functional applications has significant potential that may lead to advances in treatment strategies. While the precise mechanisms of action are yet to be elucidated, *h*PM has been shown to play a key role in angiogenesis and immune regulation. Used as either a discrete 'active' biomaterial or as a composite, continued development may lead to alternative strategies for clinical revascularization and organ regeneration.

5. Conclusions

A human extracellular matrix containing angiogenic and immunoregulatory cytokines is shown to induce *in vitro* and *in vivo* angiogenesis within engineered biomaterials while inhibiting implant fibrosis. Implementation of *h*PM provides an alternative to Matrigel and, due to its human derivation, may provide a platform for the development of clinically applicable therapeutic angiogenic or vasculogenic techniques that avoid significant immunological and inflammatory reactions. These positive outcomes may be explained, in part, not only by the presence of key growth factors (GF) and gene regulators but also their presence in physiological ratios obtained through the purification process.

Disclosures

None.

Acknowledgments

The authors are thankful for the financial support provided by the National Institute of Health (NIH R01 HL088207). In addition, the authors would like to thank Aurore Van de Walle for assistance in scanning electron microscopy.

Appendix A. Supplementary data

Supplementary data related to this article can be found online at http://dx.doi.org/10.1016/j.biomaterials.2015.01.022.

References

[1] Jain RK, Schlenger K, Hockel M, Yuan F. Quantitative angiogenesis assays: progress and problems. Nat Med 1997;3:1203–8.
[2] Staton CA, Stribbling SM, Tazzyman S, Hughes R, Brown NJ, Lewis CE. Current methods for assaying angiogenesis in vitro and in vivo. Int J Exp Pathol 2004;85:233–48.
[3] Stokes CL, Lauffenburger DA. Analysis of the roles of microvessel endothelial cell random motility and chemotaxis in angiogenesis. J Theor Biol 1991;152:377–403.
[4] Thurston G, Murphy TJ, Baluk P, Lindsey JR, McDonald DM. Angiogenesis in mice with chronic airway inflammation: strain-dependent differences. Am J Pathol 1998;153:1099–112.
[5] Cristofanilli M, Charnsangavej C, Hortobagyi GN. Angiogenesis modulation in cancer research: novel clinical approaches. Nat Rev Drug Discov 2002;1:415–26.
[6] Lokmic Z, Mitchell GM. Engineering the microcirculation. Tissue Eng Part B Rev 2008;14:87–103.
[7] Kurz H, Burri PH, Djonov VG. Angiogenesis and vascular remodeling by intussusception: from form to function. News Physiol Sci: Int J Physiol Prod Int Union Physiol Sci Am Physiol Soc 2003;18:65–70.
[8] Burri PH, Djonov V. Intussusceptive angiogenesis–the alternative to capillary sprouting. Mol Aspects Med 2002;23:S1–27.
[9] Risau W. Mechanisms of angiogenesis. Nature 1997;386:671–4.
[10] Folkman J. Angiogenesis in cancer, vascular, rheumatoid and other disease. Nat Med 1995;1:27–31.
[11] Auerbach R, Akhtar N, Lewis RL, Shinners BL. Angiogenesis assays: problems and pitfalls. Cancer Metastasis Rev 2000;19:167–72.
[12] Warren MS, Zerangue N, Woodford K, Roberts LM, Tate EH, Feng B, et al. Comparative gene expression profiles of ABC transporters in brain microvessel endothelial cells and brain in five species including human. Pharmacol Res 2009;59:404–13.
[13] Febbraio M, Hajjar DP, Silverstein RL. CD36: a class B scavenger receptor involved in angiogenesis, atherosclerosis, inflammation, and lipid metabolism. J Clin Invest 2001;108:785–91.
[14] Zisch AH, Lutolf MP, Hubbell JA. Biopolymeric delivery matrices for angiogenic growth factors. Cardiovasc Pathol 2003;12:295–310.
[15] Ehrbar M, Zeisberger SM, Raeber GP, Hubbell JA, Schnell C, Zisch AH. The role of actively released fibrin-conjugated VEGF for *VEGF receptor 2* gene activation and the enhancement of angiogenesis. Biomaterials 2008;29:1720–9.
[16] Lutolf M, Hubbell J. Synthetic biomaterials as instructive extracellular microenvironments for morphogenesis in tissue engineering. Nat Biotechnol 2005;23:47–55.
[17] Cockerill GW, Gamble JR, Vadas MA. Angiogenesis: models and modulators. Int Rev Cytol 1995;159:113–60.
[18] Kleinman HK, Martin GR. Matrigel: basement membrane matrix with biological activity. Semin Cancer Biol 2005;15:378–86.
[19] Auerbach R, Lewis R, Shinners B, Kubai L, Akhtar N. Angiogenesis assays: a critical overview. Clin Chem 2003;49:32–40.
[20] Wang Y, Zhao S. Vascular biology of the placenta. San Rafael (CA). 2010.
[21] Jaffe EA, Nachman RL, Becker CG, Minick CR. Culture of human endothelial cells derived from umbilical veins. Identification by morphologic and immunologic criteria. J Clin Invest 1973;52:2745.
[22] Daniel J, Abe K, McFetridge PS. Development of the human umbilical vein scaffold for cardiovascular tissue engineering applications. ASAIO J 2005;51:252–61.
[23] Fett JW, Strydom DJ, Lobb RR, Alderman EM, Bethune JL, Riordan JF, et al. Isolation and characterization of angiogenin, an angiogenic protein from human carcinoma cells. Biochemistry 1985;24:5480–6.
[24] Xu J, Rodriguez D, Petitclerc E, Kim JJ, Hangai M, Yuen SM, et al. Proteolytic exposure of a cryptic site within collagen type IV is required for angiogenesis and tumor growth in vivo. J Cell Biol 2001;154:1069–80.
[25] Kim S, Bell K, Mousa SA, Varner JA. Regulation of angiogenesis *in vivo* by ligation of integrin α5β1 with the central cell-binding domain of fibronectin. Am J Pathol 2000;156:1345–62.
[26] Iozzo RV, San Antonio JD. Heparan sulfate proteoglycans: heavy hitters in the angiogenesis arena. J Clin Invest 2001;108:349–55.
[27] Patarroyo M, Tryggvason K, Virtanen I. Laminin isoforms in tumor invasion, angiogenesis and metastasis. Seminars in cancer biology. Elsevier; 2002. p. 197–207.
[28] Rundhaug JE. Matrix metalloproteinases and angiogenesis. J Cell Mol Med 2005;9:267–85.
[29] Kalluri R. Basement membranes: structure, assembly and role in tumour angiogenesis. Nat Rev Cancer 2003;3:422–33.
[30] Nör J, Mitra RS, Sutorik MM, Mooney DJ, Castle VP, Polverini PJ. Thrombospondin-1 induces endothelial cell apoptosis and inhibits angiogenesis by activating the caspase death pathway. J Vasc Res 2000;37:209–18.
[31] Laschke MW, Harder Y, Amon M, Martin I, Farhadi J, Ring A, et al. Angiogenesis in tissue engineering: breathing life into constructed tissue substitutes. Tissue Eng 2006;12:2093–104.
[32] Nerem RM, Seliktar D. Vascular tissue engineering. Annu Rev Biomed Eng 2001;3:225–43.
[33] Perretti M, Chiang N, La M, Fierro IM, Marullo S, Getting SJ, et al. Endogenous lipid-and peptide-derived anti-inflammatory pathways generated with glucocorticoid and aspirin treatment activate the lipoxin A4 receptor. Nat Med 2002;8:1296–302.
[34] Paslakis G, Keuneke C, Groene H-J, Schroppel B, Schmid H, Schloendorff D. The putative role of human peritoneal adipocytes in the fight against bacteria: synthesis of the antimicrobial active peptide DEFA1-3. Nephron Exp Nephrol 2010;115:e96–100.
[35] Kim SJ, Ruiz N, Bezouška K, Drickamer K. Organization of the gene encoding the human macrophage mannose receptor (MRC1). Genomics 1992;14:721–7.
[36] Place ES, Evans ND, Stevens MM. Complexity in biomaterials for tissue engineering. Nat Mater 2009;8:457–70.
[37] Lee S-H, Tseng S. Amniotic membrane transplantation for persistent epithelial defects with ulceration. Am J Ophthalmol 1997;123:303–12.
[38] Jin CZ, Park SR, Choi BH, Lee K-Y, Kang CK, Min B-H. Human amniotic membrane as a delivery matrix for articular cartilage repair. Tissue Eng 2007;13:693–702.
[39] Bose B. Burn wound dressing with human amniotic membrane. Ann R Coll Surg Engl 1979;61:444.
[40] Adair T. Angiogenesis. Integrated systems physiology, from molecule to function to disease. Morgan & Claypool; 2011.
[41] Djonov V, Baum O, Burri PH. Vascular remodeling by intussusceptive angiogenesis. Cell Tissue Res 2003;314:107–17.
[42] Vailhe B, Vittet D, Feige JJ. In vitro models of vasculogenesis and angiogenesis. Lab Invest J Tech Methods Pathol 2001;81:439–52.
[43] Pepper M, Ferrara N, Orci L, Montesano R. Potent synergism between vascular endothelial growth factor and basic fibroblast growth factor in the induction of angiogenesis in vitro. Biochem Biophys Res Commun 1992;189:824–31.
[44] Sullivan DC, Bicknell R. New molecular pathways in angiogenesis. Br J Cancer 2003;89:228–31.
[45] O'Byrne KJ, Dalgleish A, Browning M, Steward W, Harris A. The relationship between angiogenesis and the immune response in carcinogenesis and the progression of malignant disease. Eur J Cancer 2000;36:151–69.
[46] Epstein SE, Fuchs S, Zhou YF, Baffour R, Kornowski R. Therapeutic interventions for enhancing collateral development by administration of growth factors: basic principles, early results and potential hazards. Cardiovasc Res 2001;49:532–42.
[47] Lee RJ, Springer ML, Blanco-Bose WE, Shaw R, Ursell PC, Blau HM. VEGF gene delivery to myocardium deleterious effects of unregulated expression. Circulation 2000;102:898–901.
[48] Hariawala MD, Horowitz JR, Esakof D, Sheriff DD, Walter DH, Keyt B, et al. VEGF improves myocardial blood flow but produces EDRF-mediated hypotension in porcine hearts. J Surg Res 1996;63:77–82.
[49] Montesano R, Vassalli J-D, Baird A, Guillemin R, Orci L. Basic fibroblast growth factor induces angiogenesis in vitro. Proc Natl Acad Sci 1986;83:7297–301.
[50] Ferrara N, Alitalo K. Clinical applications of angiogenic growth factors and their inhibitors. Nat Med 1999;5.